JOURNAL OF CATALYSIS 136, 539–553 (1992)

Surface Structures of Supported Molybdenum Oxide Catalysts under Ambient Conditions

DU SOUNG KIM,* KOICHI SEGAWA,† TOMOTSUNE SOEYA,† AND ISRAEL E. WACHS†,[1]

*Zettlemoyer Center for Surface Studies, Department of Chemical Engineering, Lehigh University, Bethlehem, Pennsylvania 18015; and †Department of Chemistry, Faculty of Science and Technology, Sophia University, 7-1 Kioi-cho, Chiyoda-ku, Tokyo 102 Japan

Received December 6, 1991; revised March 4, 1992

Two sets of supported molybdenum oxide catalysts, wet (dried at room temperature) and calcined (calcined at 773 K) samples, were prepared by an equilibrium adsorption method at different pH values of the impregnating solution. The adsorbed amounts of molybdenum oxide species onto the oxide support are strongly dependent on the pH of the impregnating solution and increase with decreasing pH. The Raman spectroscopic studies reveal that the surface molybdenum oxide species under ambient conditions, wet and calcined, are hydrated and essentially in an aqueous medium. Furthermore, the surface structures of molybdenum oxide species on the oxide support were found to depend on the net surface pH at point of zero charge (PZC) under ambient conditions. The net surface pH at PZC under ambient conditions is determined by the specific oxide support and surface molybdenum oxide coverage. The surface molybdenum oxide structures in the wet, uncalcined, samples are not only dependent on the net surface pH at PZC but also on the number of NH_4^+ cations which coordinate to the surface molybdenum oxide species for compensation of net charge: $Mo_7O_{24}^{6-}$ species in NH_4^+-rich concentrations (high pH region) favor formation of $(NH_4)_6Mo_7O_{24} \cdot 4H_2O$. Upon calcination, the NH_4^+ ions are removed and the surface molybdenum oxide species become rehydrated upon exposure to air by adsorbing moisture. Consequently, the structures of surface molybdenum oxide species in the calcined samples which have been exposed to ambient are also dependent on the net surface pH at PZC.

INTRODUCTION

Molybdenum oxide catalysts are very important catalysts in the petrochemical industry. These catalysts are usually used by supporting the catalytically active species (molybdenum oxide species) on an inorganic oxide support (TiO_2, ZrO_2, Al_2O_3, SiO_2, and MgO) for the purpose of (1) increasing the catalytic activity and selectivity, (2) extending the life of the catalysts, and (3) increasing the mechanical strength of the catalysts. A few studies have investigated the effect of the oxide support on the surface properties (*1–4*) and catalytic activities of supported molybdenum oxide catalysts (*5–11*). It was concluded that the surface properties of molybdenum oxide species are strongly influenced by the oxide support type and result in different catalytic behavior.

The industrial importance of supported molybdenum oxide catalysts in numerous catalytic applications has prompted a large number of studies concerning the surface structures of molybdenum oxide catalysts by Fourier transform infrared (FTIR) (*12*a, *13*a), ultraviolet visible diffuse reflectance (*13*a,b, *14–16*), extended X-ray absorption fine structure (EXAFS) (*17–22*a), X-ray absorption near edge structure (XANES) (*19, 20*), solid-state ^{95}Mo nuclear magnetic resonance (NMR) (*23–26*), and Raman (*12*a, *13*a,c, *14, 16, 19, 22, 26–38*) spectroscopies. Raman spectroscopy has probably been the greatest contributor to the rapid progress in this area of catalysis because of its ability to discriminate between different

[1] To whom correspondence should be addressed.

0021-9517/92 $5.00

metal oxide structures and its *in situ* capabilities.

A number of studies on the assignment of Raman band positions have been reported (*12*a, *13*a,c *14, 16, 19, 22, 26–38*). However, there are still disagreements on the interpretation of Raman band shifts which occur as the molybdenum oxide content increases. Ng and Gulari (*12*a) have proposed that the bands at 955 cm^{-1} or at lower wavenumbers can be attributed to the terminal Mo=O bonds of the isolated tetrahedral species and that the bands above 955 cm^{-1} are due to the polymeric octahedral species. A similar interpretation of Raman band shifts with increasing molybdenum oxide content have also been reported by Wang and Hall (*13*a,c) and Sombret *et al.* (*35*). Kim *et al.* (*26*) and Brown *et al.* (*31*) have concluded that the Raman bands observed at 930–970 cm^{-1} are attributed to the octahedrally coordinated polymolybdate species. Iannibello *et al.* (*38*) have suggested that the Raman band at 940 cm^{-1} is due to the symmetric Mo=O stretching of MoO_4^{2-} in tetrahedral coordination, while the Raman band shifts to higher wavenumber could reflect distortion of the tetrahedral symmetry. Most of the previous conclusions regarding on the surface structures of the supported molybdenum oxide catalysts are contradictory and necessitate a systematic study on the nature of supported molybdenum oxide catalysts.

Supported molybdenum oxide catalysts are usually prepared by coprecipitation, impregnation, and/or incipient-wetness methods. Recently, an equilibrium adsorption method was devised to prepare the highly dispersed metal oxide species on the oxide support (*13, 26*). In this method, molybdate anions are made to adsorb onto positively charged oxide support surfaces, via electrostatic attraction, by controlling the pH of the impregnating solution. Moreover, the adsorbed amounts of molybdenum oxide species are controlled by the pH of the impregnating solution because the number of positively charged sites on the oxide support surface are governed by the pH of the impregnating solution. Deo and Wachs (*27*) have proposed that under ambient conditions the surface of the oxide support is hydrated and surface metal oxide (V_2O_5, Re_2O_7, MoO_3, CrO_3, or WO_3) overlayers are essentially in an aqueous medium. Consequently, the structure of the metal oxide overlayer follows the metal oxide aqueous chemistry as a function of the net pH at the point of zero charge (PZC) and metal oxide concentration. Therefore, the pH of the impregnating solution and the pH at the PZC oxide support may also be important parameters in the regulation of the surface properties of supported molybdenum oxide species.

In the present investigation, we report the effects of the oxide supports, pH of the impregnating solution (surface molybdenum oxide content), and impurities present on the oxide support on the molecular structures of surface molybdenum oxide species under ambient conditions. The objectives of this study were to determine the molecular structures of the hydrated surface molybdenum oxide species, the Raman band assignments, and the influence of the preparation method and oxide supports.

EXPERIMENTAL

Catalyst preparation. The supported molybdenum oxide catalysts were prepared by the equilibrium adsorption method with aqueous solutions of ammonium heptamolybdate ($(NH_4)_6Mo_7O_{24} \cdot 4H_2O$) (*13, 26*). The support materials used in this study were TiO_2 (anatase) (Idemitsu, UFP-TiO_2,), SiO_2 (Degussa, Aerosil-200), TiO_2 (rutile) (JRC-TiO-3), Al_2O_3 (JRC-ALO-4), MgO (JRC-MgO-1), and ZrO_2. The TiO_2 (rutile), Al_2O_3, and MgO supports employed were Japan Reference Catalysts (JRC) (*39*) and ZrO_2 was prepared by the method of Tanabe and co-workers (*40*). The TiO_2 (anatase) support was obtained by calcining the amorphous Idemitsu UFP TiO_2 at 773 K for 2 h. The catalysts were prepared by shaking a suspension of 5 g of the support at 323 K for 100 h in 0.007 *M* aqueous solution of ammo-

nium heptamolybdate (analytical grade). The pH of the suspended solution was continuously adjusted with a dilute solution of HNO_3 or NH_4OH. After adsorption, the wet solid was separated from the solution by filtration, dried at room temperature (wet samples), dried at 373 K for 12 h, and then calcined 773 K for 12 h (calcined samples). The adsorbed amounts of molybdenum as oxide base (wt% MoO_3) were determined by Inductive Coupled Plasma Emission Spectroscopy (ICPES, Seiko Denshi, SPS-1100). For ICPES measurement, 200 mg of the sample was fused with K_2SO_4 and dissolved with diluted H_2SO_4 solution.

BET surface area and CO_2 chemisorption. Both experiments were performed in a standard BET adsorption system. Prior to the measurement, the samples were treated with O_2 at 773 K for 1 h and then evacuated at the same temperature for 0.5 h. BET surface areas of the catalysts were determined by N_2 adsorption at 77 K. CO_2 adsorption isotherms of the catalysts were measured at 293 K. Adsorption isotherms of the Langumuir type have been obtained for all catalysts. The CO_2 chemisorption of each catalyst was determined at the extrapolated pressure of zero.

Raman spectroscopy. Raman spectroscopy of supported molybdenum oxide catalysts, wet and calcined samples, under ambient conditions were obtained with an Ar^+ laser (Spectra Physics, Model 171). The incident laser line was 514.5 nm and delivered 10–20 mW of power measured at the sample. The scattered radiation from the sample was directed into a Spex Triplemate spectrometer (model 1877) coupled to a Princeton Applied Research OMA III optical multichannel analyzer (model 1463) equipped with an intensified photodiode array detector cooled thermoelectrically to 243 K. The Raman spectra were collected and recorded using an OMA III (PAR) directed computer and software. The spectral resolution and reproducibility was experimentally determined to be better than 2 cm^{-1}. About 0.1–0.2 g of each supported molybdenum oxide catalyst was pressed into a thin wafer of about 1 mm thickness. Each sample was then mounted onto a spinning sample holder and rotated at ~2000 rpm to avoid local heating effect by laser.

TABLE 1

Surface Properties of Oxide Supports

Oxide support	PZC[a] (pH)	Specific surface area ($m^2\ g^{-1}$)	CO_2 uptake ($\mu mol\ g^{-1}$)
TiO_2 (anatase)	6.2	68.5	197.0
TiO_2 (rutile)	4.7 ~ 5.5[b]	48.4	107.0
ZrO_2	6.7	54.8	336.0
Al_2O_3	6.0 ~ 8.9[b]	165.0	193.0
SiO_2	1.8 ~ 3.9[b]	160.0	14.8
MgO	12.4	58.6	196.0

[a] Reference (*27*).
[b] References (*27, 41*).

RESULTS

The surface properties of the oxide supports are presented in Table 1. As stated previously, they are important parameters in the regulation of the surface properties of supported molybdenum oxide species. The surface hydroxyl groups of the support in solution tend to polarize and to be electrically charged. The pH value at which the net surface charge (or zeta potential) of the support is zero corresponds to its point of zero charge (PZC) or its isoelectric point (IEP) (*41*). As shown in Table 1, the different oxide supports possess different pH values at PZC. The SiO_2 and MgO supports possess low and high pH values at point of zero charge (PZC), respectively. The TiO_2 (anatase), TiO_2 (rutile), ZrO_2, and Al_2O_3 supports exhibit neutral pH at PZC. The surface area of TiO_2 (anatase), TiO_2 (rutile), ZrO_2, Al_2O_3, SiO_2, and MgO were 68.5, 48.4, 54.8, 165.0, 160, and 58.6 m^2g^{-1}, respectively. It is well established that CO_2 chemisorbs selectively on the oxide support surface but does not show any interaction with surface molybdenum oxide species (*26,*

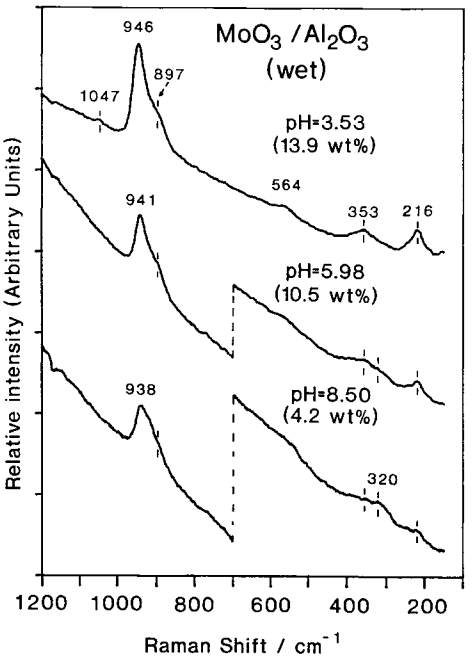

FIG. 1. The Raman spectra of wet MoO_3/Al_2O_3 under ambient conditions at different pH values.

42, 43). The SiO_2 support shows extremely low CO_2 uptakes compared to the other supports due to the low surface hydroxyl density because of the ease formation of siloxane linkage (Si–O–Si) on dehydroxylation during calcination by O_2 at 773 K before CO_2 chemisorption.

MoO_3/Al_2O_3 Catalysts

The Raman spectra of the wet and calcined MoO_3/Al_2O_3 samples under ambient conditions, where the samples contain adsorbed moisture, are presented in Figs. 1 and 2 as a function of the pH of the impregnating solution. The Raman spectra of the wet samples are shown in Fig. 1. The samples prepared at a pH of 5.98 (10.5 wt%) and above possess Raman bands at 938–941, ~897, ~564, ~353, ~320, and 216 cm^{-1}. The bands observed at 938–941, ~897, and ~353 cm^{-1} are attributed to the symmetric and asymmetric stretching, and bending mode of the terminal Mo=O bond of octahedrally coordinated $Mo_7O_{24}^{6-}$ species, respectively (*12*b,c, *13*a,c, *44*). In addition, the bands at ~564 and 216 cm^{-1} are assigned to the Mo–O–Mo symmetric stretches and Mo–O–Mo deformations of $Mo_7O_{24}^{6-}$ species, respectively. The Raman band at ~320 cm^{-1} is due to the Mo–O bending mode of isolated and tetrahedrally coordinated MoO_4^{2-} species (*12, 13*). The symmetric stretching mode of MoO_4^{2-} (894 cm^{-1}) overlaps the band of the asymmetric mode of $Mo_7O_{24}^{6-}$ at ~897 cm^{-1}. The Raman band due to the MoO_4^{2-} species (~320 cm^{-1}) disappears and the bands attributed to the $Mo_7O_{24}^{6-}$ species predominate in the spectrum of the pH = 3.53 (13.9 wt%) sample. The very weak Raman band corresponding to NO_3^- appears at ~1047 cm^{-1} (*13*a,c) for the sample prepared at low pH (pH = 3.53, 13.9 wt%) since HNO_3 is added to the impregnating solution in order to lower the pH of the impregnating solution during preparation.

The Raman spectra of the calcined MoO_3–Al_2O_3 samples, under ambient condi-

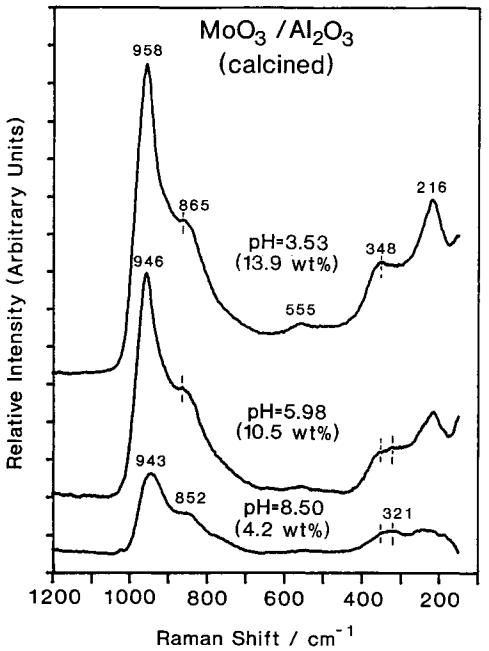

FIG. 2. The Raman spectra of calcined MoO_3/Al_2O_3 under ambient conditions at different pH values.

tions, are presented in Fig. 2. The pH = 8.50 (4.2 wt%) sample exhibits Raman bands at 943, ~348, and 216 cm^{-1} due to the $Mo_7O_{24}^{6-}$ species and the band at ~320 cm^{-1} for the MoO_4^{2-} species. These results indicate that $Mo_7O_{24}^{6-}$ and MoO_4^{2-} species coexist on the alumina surface after preparation at high pH values (low molybdenum oxide contents). The upward shift of the symmetric stretching mode of the terminal Mo=O band to 958 cm^{-1} for the pH = 3.53 (13.9 wt%) sample suggests that the $Mo_8O_{26}^{4-}$ species is predominant at the lower pH region. The calcined samples also possess Raman bands at 852–865 cm^{-1} which might be due to stretching mode of Mo–O–Mo bond (see discussion below). The Raman bands due to the asymmetric stretching modes of the terminal Mo=O bonds for $Mo_7O_{24}^{6-}$ (903 cm^{-1}) and $Mo_8O_{26}^{4-}$ (925 cm^{-1}) are obscured by the bands of the symmetric stretching mode of terminal Mo=O (948–958 cm^{-1}) and asymmetric stretching mode of Mo–O–Mo (852–865 cm^{-1}).

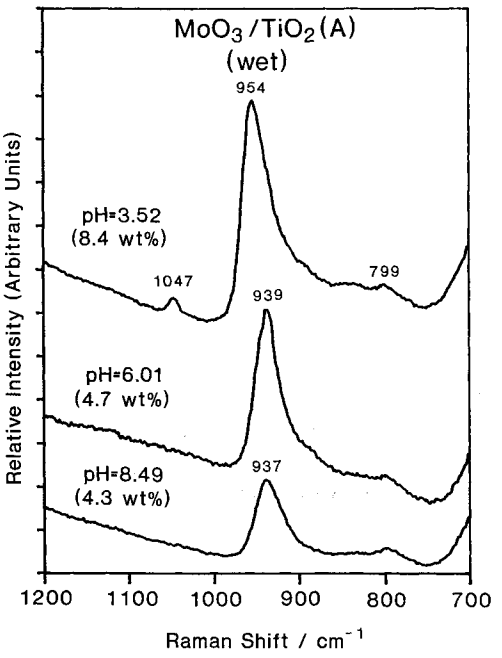

FIG. 3. The Raman spectra of wet MoO_3/TiO_2 (anatase) under ambient conditions at different pH values.

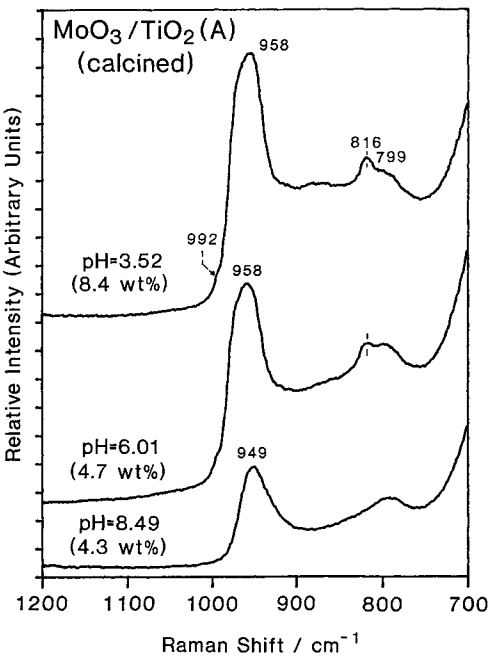

FIG. 4. The Raman spectra of calcined MoO_3/TiO_2 (anatase) under ambient conditions at different pH values.

MoO_3/TiO_2 (Anatase) Catalysts

The Raman spectra of the wet and calcined MoO_3/TiO_2 (anatase) samples under ambient conditions are shown in Figs. 3 and 4. The strong support Raman features due to the TiO_2 (anatase) phase limit the collection of the data below 700 cm^{-1}. The wet samples exhibit Raman bands at 937, 939, and 954 cm^{-1} for the samples prepared at pH = 8.49 (4.3 wt%), pH = 6.01 (4.7 wt%), and pH = 3.52 (8.4 wt%), respectively. The weak band at 799 cm^{-1} is assigned to the first overtone of the 395 cm^{-1} band of TiO_2 (anatase). The Raman bands observed at 937–939 cm^{-1} originate from the symmetric stretching mode of terminal Mo=O of the octahedrally coordinated molybdenum oxide species ($Mo_7O_{24}^{6-}$). The band position of the terminal Mo=O bond for MoO_3/TiO_2 prepared at a pH above 6.01 (4.7 wt%) is slightly lower than the octahedrally coordinated species such as aqueous $Mo_7O_{24}^{6-}$ (943 cm^{-1}) and slightly higher than that of

$(NH_4)_6Mo_7O_{24} \cdot 4H_2O$ (934 cm^{-1}). The wet samples prepared at the high pH region possess more NH_4^+ ions than those prepared at the low pH region because NH_4OH is added to the impregnating solution in order to increase the pH. Therefore, some of the surface molybdenum oxide species, $Mo_7O_{24}^{6-}$, present in the wet samples prepared at the high pH region are stabilized by the NH_4^+ ions. This result suggests that the number of NH_4^+ ions which coordinate to the molybdenum oxide species may influence the surface molybdenum oxide species. Moreover, the broadening of the terminal Mo=O bond for the samples prepared at the high-pH region suggests that both $Mo_7O_{24}^{6-}$ and $(NH_4)_6Mo_7O_{24} \cdot 4H_2O$ probably coexist on the TiO_2 (anatase) surface. The band observed at 954 cm^{-1} for the sample prepared at pH = 3.52 (8.4 wt%) suggests that $Mo_8O_{28}^{4-}$ is the predominant species on the titania (anatase) surface. The Raman band due to the NO_3^- is also observed at 1047 cm^{-1} for the sample prepared at low pH (pH = 3.52 (8.4 wt%)).

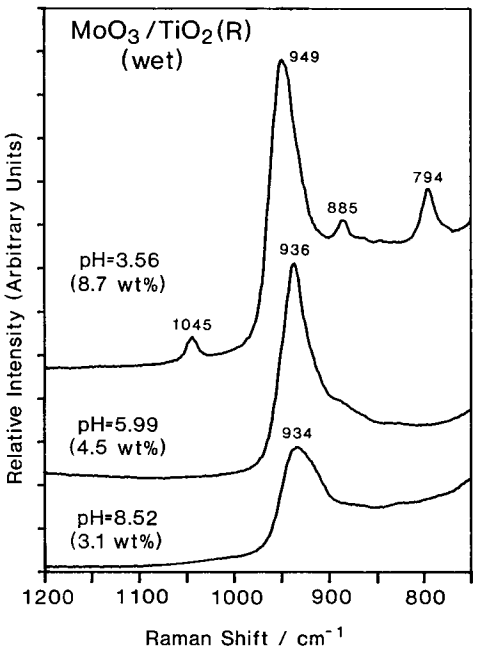

FIG. 5. The Raman spectra of wet MoO_3/TiO_2 (rutile) under ambient conditions at different pH values.

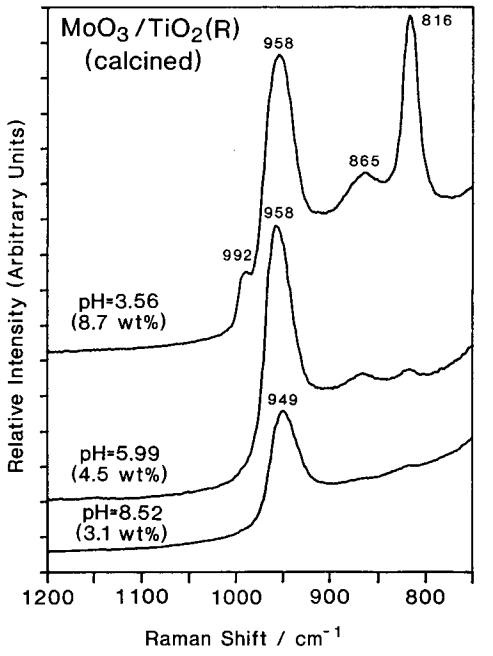

FIG. 6. The Raman spectra of calcined MoO_3/TiO_2 (rutile) under ambient conditions at different pH values.

The Raman spectra of the calcined MoO_3/TiO_2 (anatase) samples under ambient conditions are presented in Fig. 4. The calcined samples possess Raman bands due to polymolybdate species, $Mo_7O_{24}^{6-}$ and/or $Mo_8O_{28}^{4-}$, in the 949–958 cm^{-1} region. The samples prepared at pH = 3.52 (8.4 wt%) and pH = 6.01 (4.7 wt%) possess very weak Raman bands at 816 and 992 cm^{-1} characteristic of crystalline MoO_3 particles. Therefore, the samples prepared at a pH below 6.01 (4.7 wt%) possess slightly more than monolayer coverage of surface molybdenum oxide.

MoO_3/TiO_2 (Rutile) Catalysts

The Raman spectra of the wet and calcined MoO_3/TiO_2 (rutile) samples under ambient conditions are presented in Figs. 5 and 6. The strong support Raman bands below 700 cm^{-1} interfere with the detection of diagnostic Raman bands for the other molybdate functionalities. As shown in Fig. 5, the wet samples prepared at a pH of 5.99 (4.5 wt%)

and above exhibit a Raman band in the 934–936 cm^{-1} region. The Raman band position of the terminal Mo=O bond for the samples prepared at a pH of 5.99 (4.5 wt%) and above falls in the region observed for $(NH_4)_6Mo_7O_{24} \cdot 4H_2O$ (934 cm^{-1}). This result suggests that $(NH_4)_6Mo_7O_{24} \cdot 4H_2O$ predominates at the high-pH region. The broadening of the terminal Mo=O bond for the samples prepared at the high-pH region indicates the presence of $Mo_7O_{24}^{6-}$ species as well as $(NH_4)_6Mo_7O_{24} \cdot 4H_2O$. The shift in the Raman band to higher wavenumber (949 cm^{-1}) on decreasing the pH to 3.56 (8.7 wt%) is attributed to the increase in the ratio of $Mo_8O_{26}^{4-}/Mo_7O_{24}^{6-}$. The sample prepared at pH = 3.56 (8.7 wt%) also exhibits additional Raman features at 885 and 794 cm^{-1}. These bands disappear in the calcined samples and give strong crystalline MoO_3 bands at 816 and 992 cm^{-1} (see Fig. 6). Therefore, it appears that these bands may be related to the precursor of the crystalline MoO_3 phase. The Raman band due to the No_3^- is also observed at 1045 cm^{-1} for the sample prepared at pH = 3.56 (8.7 wt%).

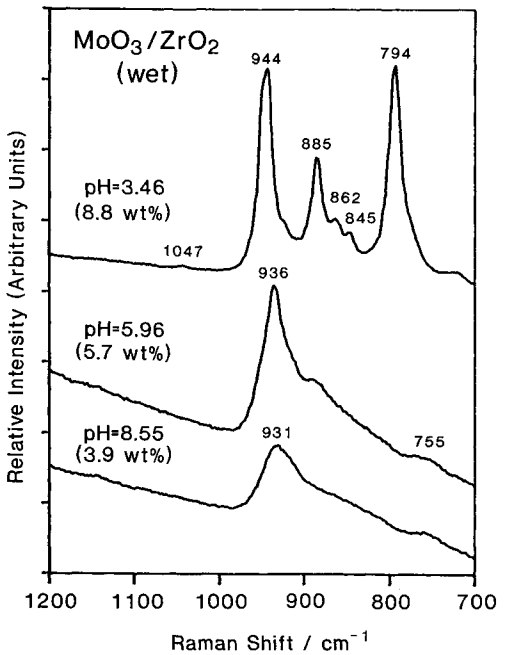

FIG. 7. The Raman spectra of wet MoO_3/ZrO_2 under ambient conditions at different pH values.

The Raman spectra of the corresponding calcined samples are shown in Fig. 6. The calcined sample prepared at pH = 8.52 (3.1 wt%) shows a major Raman band for the surface molybdate species ($Mo_7O_{24}^{6-}$ and/or $Mo_8O_{26}^{4-}$) at 949 cm^{-1}. The Raman band at 958 cm^{-1} for the samples prepared at a pH of 5.99 (4.5 wt%) and below suggest that $Mo_8O_{26}^{4-}$ species are mainly present on the TiO_2 (rutile) surface. Moreover, these samples also exhibit Raman bands for the crystalline MoO_3 at 816 and 992 cm^{-1} as well as a Raman band at ~865 cm^{-1} for the stretching mode of Mo–O–Mo bond (see discussion below). The Raman bands due to the asymmetric stretching modes of the terminal Mo=O bonds for $Mo_7O_{24}^{6-}$ and $Mo_8O_{26}^{4-}$ are obscured by the bands of symmetric Mo=O and asymmetric Mo–O–Mo bonds.

MoO_3/ZrO_2 Catalysts

The Raman spectra of the wet and calcined MoO_3/ZrO_2 samples under ambient conditions are shown in Figs. 7 and 8. The Raman spectra below 700 cm^{-1} were not collected because the strong scattering from the ZrO_2 support dominates this region. The weak Raman band due to the ZrO_2 substrate is observed at 755 cm^{-1}. The wet MoO_3/ZrO_2 samples (Fig. 7) prepared at a pH above 5.96 (5.7 wt%) exhibit Raman bands at 931–936 cm^{-1} which is attributed to the $(NH_4)_6Mo_7O_{24}^{6-} \cdot 4H_2O$ as well as octahedrally coordinated $Mo_7O_{24}^{6-}$ species. The sample prepared at pH = 3.46 (8.8 wt%) possesses a Raman band at 944 cm^{-1} associated with the $Mo_7O_{24}^{6-}$ species and strong bands at 885 and 794 cm^{-1}, as well as two weaker bands at 862 and 845 cm^{-1} associated with the precursor of the crystalline MoO_3 phase. A weak band due to the NO_3^- is also observed for the lower pH sample (pH = 3.46, 8.8 wt%). The calcined MoO_3/ZrO_2 samples (Fig. 8) exhibit Raman bands at 945–948 cm^{-1} which are due to the polymolybdate species, $Mo_7O_{24}^{6-}$ and/or $Mo_8O_{26}^{4-}$. The catalysts prepared at a pH below 5.96

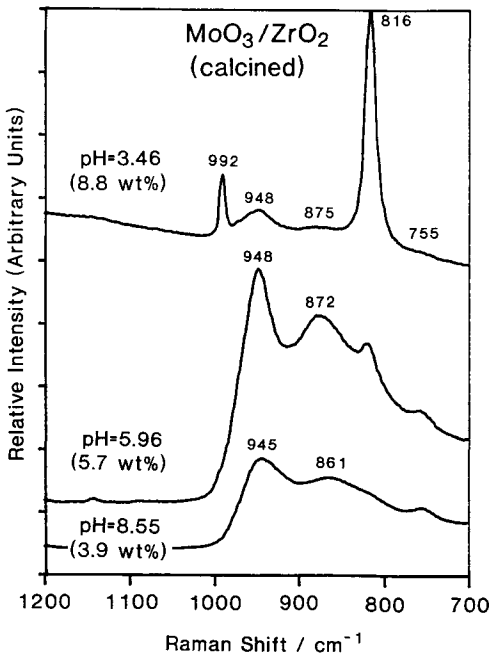

FIG. 8. The Raman spectra of calcined MoO_3/ZrO_2 under ambient conditions at different pH values.

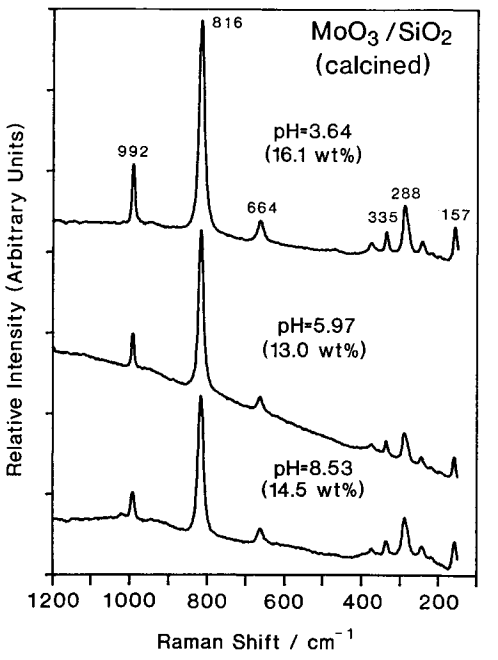

FIG. 10. The Raman spectra of calcined MoO_3/SiO_2 under ambient conditions at different pH values.

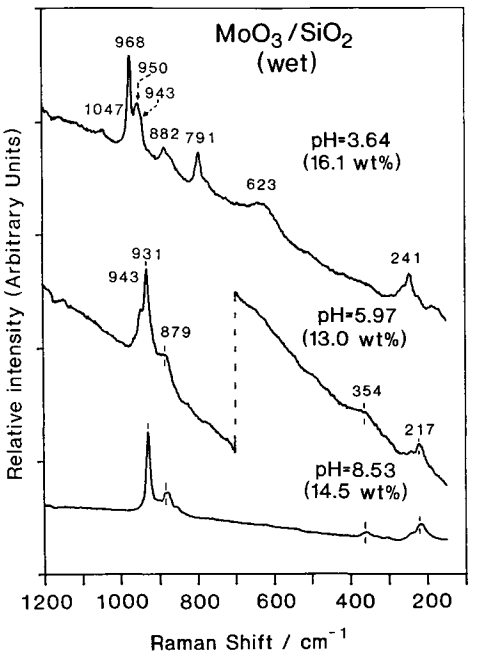

FIG. 9. The Raman spectra of wet MoO_3/SiO_2 under ambient conditions at different pH values.

(5.7 wt%) possess strong Raman bands due to the crystalline MoO_3 phase at 992 and 816 cm^{-1}. Moreover, the calcined MoO_3/ZrO_2 samples possess a broad Raman band at about 861–875 cm^{-1} due to the stretching mode of Mo–O–Mo bond (see discussion below). The Raman bands due to the asymmetric stretching modes of terminal Mo=O bonds for $Mo_7O_{24}^{6-}$ and $Mo_8O_{26}^{4-}$ are obscured by the bands of the symmetric Mo=O and the asymmetric Mo–O–Mo bonds.

MoO_3/SiO_2 Catalysts

The Raman spectra of the wet and calcined MoO_3/SiO_2 catalysts under ambient conditions are shown in Figs. 9 and 10. The Raman spectra of the wet samples at different pH values are shown in Fig. 9. The sample prepared at pH = 8.53 (14.5 wt%) possesses Raman bands at 931, ~879, ~354, 217 cm^{-1} which originate from $(NH_4)_6Mo_7O_{24} \cdot 4H_2O$ species. As the pH value decreases to 5.97 (13.0 wt%), the Raman band for the $Mo_7O_{24}^{6-}$ species (943 cm^{-1}) as well as the

Raman band for the $(NH_4)_6Mo_7O_{24} \cdot 4H_2O$ (931 cm^{-1}) are observed in the spectrum. The Raman bands due to the $(NH_4)_6Mo_7O_{24} \cdot 4H_2O$ are not present for the sample prepared at pH = 3.64 (16.1 wt%) and the Raman bands due to $Mo_7O_{24}^{6-}$ species at 943 and 217 cm^{-1} and $Mo_8O_{26}^{4-}$ species at 968 and 241 cm^{-1} predominate in the spectrum. The Raman bands for the precursor of the crystalline MoO_3 phase are also observed at 882 and 791 cm^{-1}. The calcined samples exhibit sharp and intense Raman bands of crystalline MoO_3 (992, 816, 664, 335, 288, and 157 cm^{-1}) in the spectra regardless of pH of the impregnating solution. The very weak Raman features due to the surface molybdenum oxide species ($Mo_7O_{24}^{6-}$ and/or $Mo_8O_{26}^{4-}$) are observed at about 940–960 cm^{-1}.

MoO_3/MgO Catalysts

The Raman spectra of the wet and calcined MoO_3/MgO samples under ambient conditions are shown in Figs. 11 and 12, respectively. The wet MoO_3/MgO samples exhibit Raman bands at 910, 876, 389, and 320 cm^{-1} (see Fig. 11). The band at 910 cm^{-1} is attributed to the slightly distorted, tetrahedrally coordinated MoO_4^{2-} species. The Raman bands at 876, 389, and 320 cm^{-1} correspond well with the tetrahedrally coordinated crystalline $CaMoO_4$ compound (see Fig. 13). The Raman band due to NO_3^- is observed at 1047 cm^{-1} for the pH = 8.76 (29.6 wt%) sample. As shown in Fig. 12, the calcined samples show strong Raman bands due to crystalline $CaMoO_4$ and the intensity of these bands increases as the pH value decreases. In addition, after calcination the Raman bands due to crystalline $MgMoO_4$ are also observed at 964, 949, 906, and 368 cm^{-1} and increase as the pH value decreases.

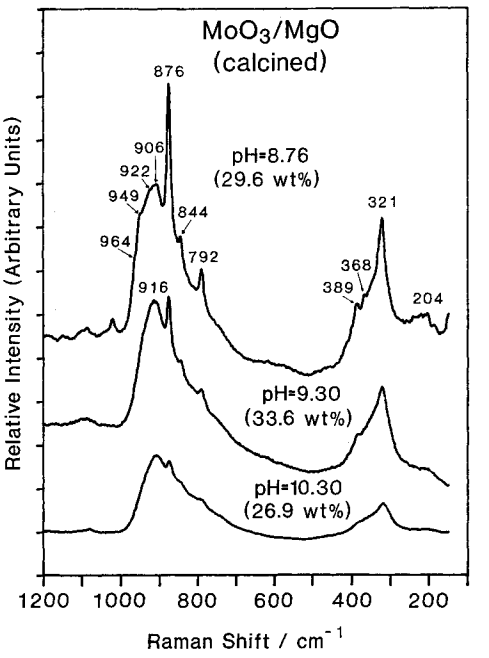

FIG. 12. The Raman spectra of calcined MoO_3/MgO under ambient conditions at different pH values.

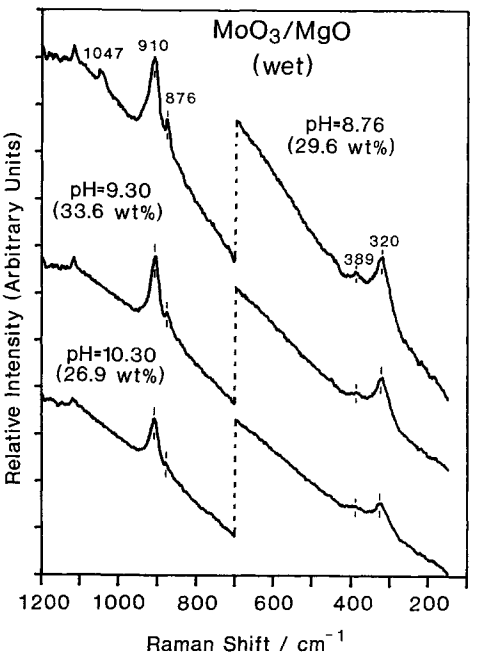

FIG. 11. The Raman spectra of wet MoO_3/MgO under ambient conditions at different pH values.

DISCUSSION

A large number of studies relating the behavior of Mo(VI) oxide species in an aqueous solution have been reported (*12*b,c, *13, 14, 25, 26, 44–46*). The molybdenum oxide

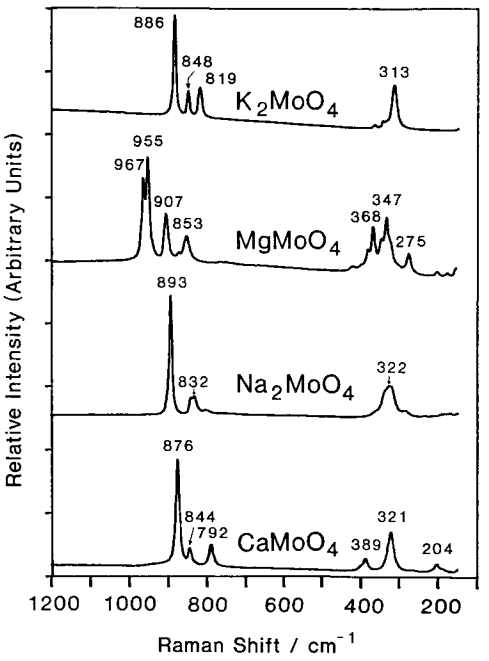

FIG. 13. The Raman spectra of tetrahedrally coordinated reference molybdenum oxide compounds under ambient conditions.

species present in an aqueous solution varies as a function of the pH of the impregnating solution (*12*b,c, *13*b,c, *25*, *26*). Wang and Hall (*13*) have reported the relationship between the pH of the impregnating solution and the molybdate species present in an aqueous solution using Raman spectroscopy. Isolated and tetrahedrally coordinated MoO_4^{2-} is the only species present in an aqueous solution at a pH above 8.0. The MoO_4^{2-} species possesses Raman bands at 897 (ν_s(Mo–O)), 837 (ν_{as}(Mo–O)), and 317 cm^{-1} (δ(Mo–O)). For pH values between 4.8 and 6.8, the predominant molybdate species is octahedrally coordinated heptamolybdate, $Mo_7O_{24}^{6-}$, with Raman bands at 943 (ν(Mo–O)), 903 (ν(Mo–O)), 362 (δ(Mo–O)), and 219 cm^{-1} (δ(Mo–O–Mo)). For pH values between 2.2 and 1.7, octahedrally coordinated β-$Mo_8O_{24}^{4-}$ species is mainly present in an aqueous solution. The β-$Mo_8O_{26}^{4-}$ anion has Raman bands at 965 (ν(Mo–O)), 925 (ν(Mo–O)), 370 (δ(Mo–O)), and 230 cm^{-1} (δ(Mo–O–Mo)). Recently, Kim *et al.* (*26*) and Luthra and Chang (*25*) have also demonstrated the pH dependence of molybdenum oxide species present in the impregnating solution by ^{95}Mo-NMR spectroscopy. It was concluded that more polymerized and complex molybdenum oxide species are present in an aqueous solution with decreasing pH of the impregnating solution. The polymerization equilibria can be explained by the following equations (*46*):

$$7MoO_4^{2-} + 8H^+ \leftrightharpoons Mo_7O_{24}^{6-} + 4H_2O \quad (1)$$

$$Mo_7O_{24}^{6-} + 3H^+ + HMoO_4^- \leftrightharpoons Mo_8O_{26}^{4-} + 2H_2O. \quad (2)$$

The Raman spectroscopic studies of the wet and calcined catalysts reveal that under ambient conditions the molybdenum oxide species present on the oxide supports are hydrated and are essentially in an aqueous medium. Consequently, the supported molybdenum oxide species resemble the molybdenum oxide species observed in an aqueous solution as a function of pH (*16*, *27*). The molybdenum oxide species of the wet samples possesses H^+ or NH_4^+ cation as counter ions in order to compensate the net charge. Therefore, the structures of the surface molybdenum oxide species of the wet samples are influenced by the ratios of NH_4^+/H^+ cations, which coordinate to the molybdenum oxide species, as well as the net surface pH at PZC. The NH_4OH buffer solution is added in order to increase the pH of the impregnating solution, and the molybdenum oxide species, $Mo_7O_{24}^{6-}$, in the NH_4^+-rich conditions (at high-pH regions) is stabilized by the NH_4^+ counterions and result in the formation of $(NH_4)_6Mo_7O_{24} \cdot 4H_2O$ (934 cm^{-1}).

The NH_4^+ ions are removed during calcination and the H^+ ions coordinate to the surface molybdenum oxide species in order to compensate for the net charge. Therefore, the molecular structures of the surface molybdenum oxide species of the calcined samples are only dependent on the net surface pH at PZC. The oxide support

with low pH at PZC such as SiO_2 (pH at PZC = 1.8 ~ 3.9) were found to favor the octahedrally coordinated polymolybdate species such as $Mo_8O_{26}^{4-}$ and/or $Mo_7O_{24}^{6-}$. The amphoteric oxide supports, TiO_2 (anatase, pH at PZC = 6.2), TiO_2 (rutile, PZC = 4.7 ~ 5.5), and ZrO_2 (pH at PZC = 6.7), favor the formation of octahedrally coordinated polymolybdate species ($Mo_7O_{24}^{6-}$ and/or $Mo_8O_{26}^{4-}$). The Al_2O_3 support (pH at PZC = 6.0 ~ 8.9) possesses both the monomeric species (MoO_4^{2-}) and polymeric species ($Mo_7O_{24}^{6-}$) at high pH values (low molybdenum oxide content), and a decrease in the pH of the impregnating solution (increase in molybdenum oxide content) results in the formation of polymolybdate species ($Mo_7O_{24}^{6-}$ and/or $Mo_8O_{26}^{4-}$). The oxide support possessing a basic aqueous pH at PZC, MgO (pH at PZC = 12.4) exhibits a preference for the formation of tetrahedrally coordinated, monomeric species like MoO_4^{2-} regardless of the pH of the impregnating solution (molybdenum oxide content). In addition, the high solubility of MgO and CaO at lower pH also results in the formation of tetrahedrally coordinated crystalline $MgMoO_4$ and $CaMoO_4$. Thus, the surface molybdenum oxide species present on oxide supports are not controlled by the solution pH during preparation, but by the surface properties of the oxide supports (surface pH at PZC).

The molybdenum oxide content also exerts an influence on the structures of adsorbed species on the oxide support under ambient conditions. The ratios of $Mo_7O_{24}^{6-}/MoO_4^{2-}$ for MoO_3/Al_2O_3 and $Mo_8O_{26}^{4-}/Mo_7O_{24}^{6-}$ for MoO_3/TiO_2 and MoO_3/ZrO_2 catalysts under ambient conditions increase as the molybdenum oxide content increases (as the pH of the impregnating solution decreases). This suggests that more polymerized molybdenum oxide species are present on the oxide support surface with increasing molybdenum oxide content which is similar to behavior of an aqueous solution at low pH. Recently, Ekerdt *et al.* (*47*) have noted that the acidic character of molybdenum and tungsten oxide in an aqueous solution results in lowering the net surface pH at PZC of the oxide support (Al_2O_3 and SiO_2). Similarly, Gil-Llambias *et al.* (*48*) have also observed that the pH at PZC for the V_2O_5/TiO_2 and V_2O_5/Al_2O_3 systems decreases as the surface vanadium oxide content increases due to the acidic properties of vanadium oxide. Recently, Vuurman and Wachs (*49*) have found that the pH at PZC of the second metal oxide, Fe_2O_3 (pH at PZC = 7 ~ 14) or MoO_3 (pH at PZC = 1.5) (*41*), also controls the molecular structures of the surface vanadium oxide overlayer on the alumina under ambient conditions. These results support the conclusion that the net surface pH at PZC is lowered by adsorption of the acidic molybdenum oxide species (*41*) and consequently, more polymerized molybdenum oxide species ($Mo_7O_{24}^{6-}$ or $Mo_8O_{26}^{4-}$) are formed upon adsorption on the oxide support surface. It is just coincidental that the amount of molybdenum oxide deposited on the supports also increases with decreasing pH of the impregnating solution.

Wang and Hall (*13*) have suggested that it is possible to control the molybdenum oxide species on the oxide supports by controlling the pH of the impregnating solution because the molybdenum oxide species present in an aqueous solution as a function of the pH adsorb intact on the oxide support surfaces. The present results reveal that *the pH of the impregnating solution does not influence structure of the surface molybdenum oxide species since this is controlled by the net surface pH at PZC.*

The calcined MoO_3/support (TiO_2, ZrO_2, and Al_2O_3) catalysts possess new Raman bands in the 865 to 875 cm^{-1} region. Hardcastle and Wachs have suggested that the bands observed at 872 cm^{-1} for MoO_3/Al_2O_3 may be due to microcrystalline molybdates formed from the cation impurities (such as K^+, Na^+, Ca^+, Sr^+, or Ba^+) present on the alumina surface since these bands are unaffected by moisture and are consistent with a regular MoO_4 tetrahedron (*28*). Ekerdt and co-workers (*16*) have reported that the for-

mation of $CaMoO_4$ is not only dependent on the Ca content of the silica support but also on the pH of the impregnating solution. They also demonstrated that the Raman spectra of MoO_3/SiO_2 prepared from $H_2(MoO_3C_2O_4) \cdot 2H_2O$ at pH = 6 contains $CaMoO_4$, whereas minimal $CaMoO_4$ is observed on samples at pH = 1.5. Although the solubility of CaO increases with decreasing pH, $CaMoO_4$ does not precipitate when silica is impregnated with $H_2(MoO_3C_2O_4)$ solutions at pH = 1.5 because the pH is too low to allow sufficient MoO_4^{2-} formation (*13, 16*). The shift and increase of the 865–875 cm^{-1} band with increasing molybdenum oxide content indicate that this band is not due to the microcrystalline molybdate species formed from the cation impurities, but due to the surface polymolybdate species. Moreover, Ekerdt *et al.* (*47*) have demonstrated that the molybdenum oxide species on SiO_2 prepared by $Mo_2(\eta^3 - C_3H_5)_4$ possesses $Mo_7O_{24}^{6-}$ species (948 and 881 cm^{-1}) under ambient conditions and isolated octahedrally coordinated molybdenum oxide species (986 cm^{-1}) under dehydrated conditions. The absence of the 881 cm^{-1} band for MoO_3/SiO_2 under dehydrated conditions is consistent with the assignment that the Raman band observed at 865–875 cm^{-1} for MoO_3/support is due to the stretching mode of the Mo–O–Mo bond of polymolybdate species on oxide supports. The 865–875 cm^{-1} band for MoO_3/supports is somewhat broad compared to that observed in the $Mo_7O_{24}^{6-}$ or $Mo_8O_{26}^{4-}$ species in aqueous solution due to the distortion caused by the interaction between the surface molybdenum oxide species and oxide supports.

It is well known that the solubility of CaO and MgO increases with decreasing pH and it is likely to make compounds with the MoO_4^{2-} species present in the aqueous solution. The wet MoO_3/MgO samples possess slightly distorted, tetrahedrally coordinated MoO_4^{2-} species as well as crystalline $CaMoO_4$ regardless of the pH of the impregnating solution. On the other hand, the calcined samples possess strong Raman bands due to the crystalline $CaMoO_4$ and $MgMoO_4$ and the intensities of these bands increase with decreasing pH of the impregnating solution. This suggests that the high solubility of MgO and impurities (CaO) in the MgO, as well as the strong acid–base interaction between MoO_4^{2-} and MgO or CaO, results in the formation of crystalline $MgMoO_4$ or $CaMoO_4$.

The adsorption processes of metal oxide species (MoO_3, Re_2O_7, WO_3, V_2O_5, and CrO_3, etc.) on high surface area oxide supports (Al_2O_{32}, TiO_2, ZrO_2, SiO_2, and MgO) have been studied by several research groups (*13, 22, 34, 38, 50–55*). Brunelle (*50*) introduced an electrostatic model to explain the adsorption of anions from solution onto metal oxide supports: charge of anions, pH of the impregnating solution, and PZC of the support are primary factors that affect adsorption. Wang and Hall (*13*) have proposed that the pH of the impregnating solution is not only a very essential parameter for regulating the amounts of adsorbed metal oxide species on the alumina surface, but also an important factor for controlling the adsorption species. They also suggested that since the metal oxide species (molybdate, tungstate, chromate, and vanadate) present in the solution are controlled by the pH of the impregnating solution that these species at a given pH are adsorbed intact on the alumina surface. Leyrer *et al.* (*51*) have proposed that the PZC of support surfaces determines the primary adsorption interaction of molybdate species with the surface at a given pH. The above models can explain the adsorption process of metal oxide species onto support surfaces, but they cannot explain the surface structures of molybdenum oxide species on the oxide support and the factors which regulate the surface metal oxide structures. Recently, Deo and Wachs (*27*) demonstrated that the net surface pH at PZC model accounts for the molecular structure of the hydrated surface vanadium oxide species on oxide supports (Al_2O_3, TiO_2, ZrO_2, SiO_2, and MgO). They also showed that the net surface pH at PZC is

determined by the specific oxide support, surface coverage of metal oxide species, impurities, calcination temperature, and acidic or basic promoters. The current work with supported molybdenum oxide catalysts shows that the net surface pH at PZC model also accounts for the behavior of molybdenum oxide catalysts.

The above concept and observed results provide an explanation for the adsorption process of molybdenum oxide species on oxide supports. The surface hydroxyls on the oxide support tend to be positively or negatively charged below or above PZC of the support (*41*). Here, S stands for the support:

$$S\text{–}OH_2^+ \underset{-H^+}{\overset{+H^+}{\rightleftharpoons}} S\text{–}OH \rightleftharpoons S\text{–}O^-. \quad (3)$$

Therefore, in agreement with Wang and Hall (*13*) and with Brunelle (*50*), the molybdenum oxide species adsorbs onto the positively charged support surface with electrostatic attraction. Moreover, the adsorbed amounts of molybdenum oxide species on the oxide support can be controlled by varying the pH of the impregnating solution. The nature of the molybdenum oxide species present on the oxide supports in the wet samples, however, are dependent on the net surface pH at PZC which is determined by the specific oxide support, the molybdenum oxide content, as well as the number of NH_4^+ and/or H^+ ions which coordinate to the surface molybdenum oxide species. Upon calcination, the NH_4^+ ions are removed and the structure of the molybdenum oxide species in the calcined samples exposed to ambient became dependent on the net surface pH at PZC.

CONCLUSIONS

The molecular structures of the molybdenum oxide overlayer on different oxide supports (TiO_2, ZrO_2, Al_2O_3, SiO_2, and MgO) were investigated using Raman spectroscopy under ambient conditions. The results reveal that the surface structures of molybdenum oxide species for the calcined MoO_3/support catalysts exposed to ambient conditions are dependent on the net surface pH at PZC. Oxide support with a low pH at PZC such as SiO_2, possess polymolybdate species such as $Mo_7O_{24}^{6-}$ and/or $Mo_8O_{26}^{4-}$ (*16, 19*). Amphoteric oxides (TiO_2 and ZrO_2) were found to prefer the $Mo_7O_{24}^{6-}$ species for low molybdenum oxide content, and the concentration of the $Mo_8O_{28}^{4-}$ species increases upon increasing the molybdenum oxide content. The Al_2O_3 support with a slightly higher pH at PZC possesses both the MoO_4^{2-} and $Mo_7O_{24}^{6-}$ species at low molybdenum oxide contents and $Mo_7O_{24}^{6-}$ and/or $Mo_8O_{26}^{4-}$ species are observed at high molybdenum oxide contents. Oxide support with a high pH at PZC such as MgO exhibits a preference for the isolated MoO_4^{2-} species regardless of molybdenum oxide content. In addition, the surface structures of molybdenum oxide species for the wet MoO_3/support catalysts are also affected by the number of NH_4^+ counter ions which coordinates to the surface molybdenum oxide species. Therefore, the surface molybdenum oxide species, $Mo_7O_{24}^{6-}$, in the NH_4^+-rich environment (high-pH region) are likely to form $(NH_4)_6Mo_7O_{24} \cdot 4H_2O$.

REFERENCES

1. Bond, G. C., Flamerz, S., and Shukri, R., *Faraday Discuss. Chem. Soc.* **87,** 65 (1989).
2. Zaki, M. I., Vielhabor, B., and Knozinger, H., *J. Phys. Chem.* **90,** 3176 (1986).
3. Nag, N. K., *J. Phys. Chem.* **91,** 2324 (1987).
4. Caceres, C. V., Fierro, J. L. G., Lazaro, J., Lopez Agudo, A., and Soria, J., *J. Catal.* **122,** 113 (1990).
5. Segawa, K., Soeya, T., and Kim, D. S., *Res. Chem. Intermediates* **15,** 129 (1991).
6. Hattori, H., Tanabe, K., Tanaka, K., and Okazaki, S., *in* "Proceedings of 3rd International Conference on the Chemistry and Uses of Molybdenum." Climax Molybdenum Co., Ann Arbor, MI, 1979.
7. Swanson, W. W., Streusand, B. J., and Tsigdinos, G. A., *in* "Proceedings of 4th International Conference on the Chemistry and Uses of Molybdenum." Climax Molybdenum Co., Golden, CO, 1982.
8. (a) Muralidhar, G., Massoth, F. E., and Shabtai, J., *J. Catal.* **85,** 44 (1984); (b) Massoth, F. E.,

Muralidhar, G., and Shabtai, J., *J. Catal.* **85,** 53 (1984).
9. Masuyama, Y., Tomatsu, Y., Ishida, K., Kurusu, Y., Segawa, K., *J. Catal.* **114,** 347 (1988).
10. Shimada, H., Sato, T., Yoshimura, Y., Hiraishi, J., Nishijima, A., *J. Catal.* **110,** 275 (1988).
11. Matsuoka, Y., Niwa, M., and Murakami,Y., *J. Phys. Chem.* **94,** 1477 (1990).
12. (a) Ng, K. Y. S., and Gulari, E., *J. Catal.* **92,** 340 (1985); (b) *J. Phys. Chem.* **89,** 2479 (1985); (c) *Polyhedron* **3,** 1001 (1984).
13. (a) Wang, L., PhD thesis, University of Wisconsin, 1982; (b) Wang, L., and Hall, W. K., *J. Catal.* **77,** 232 (1982); (c) Wang, L., and Hall, W. K., *J. Catal.* **66,** 251 (1980).
14. (a) Jeziorowski, H., and Knozinger, H., *J. Phys. Chem.* **83,** 1166 (1979); (b) *Chem. Phys. Lett.* **51,** 519 (1977).
15. Liu, Y. C., Griffin, G. L., Chan, S. S., and Wachs, I. E., *J. Catal.* **94,** 108 (1985).
16. (a) Williams, C. C., Ekerdt, J. G., Jehng, J. M., Hardcastle, F. D., Turek, A. M., and Wachs, I. E., *J. Phys. Chem.* **95,** 8781 (1991); Williams, C. C., Ekerdt, J. G., Jehng, J. M., Hardcastle, F. D., and Wachs, I. E., *J. Phys. Chem.* **95,** 8791 (1991).
17. Kakuta, N., Tohji, K., and Udagawa, Y., *J. Phys. Chem.* **92,** 2583 (1988).
18. Iwasawa, Y., Sato, Y., and Kuroda, H., *J. Catal.* **82,** 289 (1983).
19. de Boer, M., van Dillen, A. J., Konigsberger, D. C., Geus, J. W., Vuurman, M. A., and Wachs, I. E., *Catal. Lett.* **11,** 227 (1991).
20. Chieu, N. S., Bauer, S. H., and Johnson, M. F., *J. Catal.* **89,** 226 (1984); *J. Catal.* **98,** 32 (1986).
21. Clausen, B. S., Topsoe, H., Candia, R., Villadsen, J., Lengeler, B., Als-Nielsen, J., and Christiansen, F., *J. Phys. Chem.* **85,** 3868 (1981).
22. (a) van Veen, J. A. R., Hendriks, P. A. J. M., Romers, E. J. G. M., and Andrea, R. R., *J. Phys. Chem.* **94,** 5275 (1990); (b) van Veen, J. A. R., de Wit, H., Emeis, C. A., and Hendriks, P. A. J. M., *J. Catal.* **107,** 579 (1987).
23. Shirley, W. M. Z., *Phys. Chem. (Munich)* **152,** 41 (1987).
24. Edwards, J. C., and Ellis, P. D., *Langmuir* **7,** 2117 (1991); Edwards, J. C., Adams, R. D., and Ellis, P. D., *J. Am. Chem. Soc.* **112,** 8349 (1990).
25. Luthra, N. P., and Chang, W. C., *J. Catal.* **107,** 154 (1987).
26. Kim, D. S., Kurusu, Y., Wachs, I. E., Hardcastle, F. D., and Segawa, K., *J. Catal.* **120,** 325 (1989).
27. Deo, G., and Wachs, I. E., *J. Phys. Chem.* **95,** 5889 (1991).
28. Hardcastle, F. D., and Wachs, I. E., *J. Raman Spectrosc.* **21,** 683 (1990).
29. Machej, T., Haber, J., Turek, A. M., and Wachs, I. E., *Appl. Catal.* **70,** 115 (1991).
30. Stencel, J. M., Makovsky, L. E., Sarkus, T. A., de Vries, J., Thomas, R., and Moulijn, J. A., *J. Catal.* **90,** 314 (1984).
31. Brown, F. R., Makovsky, L. E., Rhee, K. H., *J. Catal.* **50,** 162 (1977).
32. Quincy, R. B., Houalla, M., Hercules, D. M., *J. Catal.* **106,** 85 (1987).
33. Cheng, C. P., and Schrader, G. L., *J. Catal.* **60,** 274 (1979).
34. (a) Kasztelan, S., Payen, E., Thoulhoat, H., Grimblot, J., and Bonnelle, J. P., *Polyhedron* **5,** 157 (1986); (b) Payen, E., Kasztelan, S., Grimblot, J., and Bonnelle, J. P., *J. Raman Spectrosc.* **17,** 233 (1986).
35. Sombret, B., Dhamelincourt, P., Wallert, F., Muller, A. C., Bouquet, M., and Grosmangin, J., *J. Raman Spectrosc.* **9,** 291 (1980).
36. Medema, J., van Stam, C., de Beer, V. J. J., Konings, A. J. A., and Koningsberger, D. C., *J. Catal.* **53,** 386 (1978).
37. Knozinger, H., and Jeziorowski, H., *J. Phys. Chem.* **82,** 2002 (1978).
38. Iannibello, A., Marengo, S., Trifiro, F., and Villa, P. L., *in* "Preparation of Catalysts II, Scientific Basis for the Preparation of Heterogeneous Catalysts" (B. Delmon, P. Grange, P. Jacobs, and G. Poncelet, Eds.), p. 65. Elsevier, Amsterdam, 1979.
39. Murakami, Y., *in* "Preparation of Catalysts III" (G. Ponceit, P. Grange, and P. A. Jacobs, Eds.), Studies in Surface Science and Catalysis Series, p. 775. Elsevier, Amsterdam, 1983.
40. Nakao, Y., Iizuka, T., Hattori, H., and Tanabe, K., *J. Catal.* **57,** 1 (1979).
41. Parks, G. A., *Chem. Rev.* **65,** 177 (1965).
42. (a) Segawa, K., and Hall, W. K., *J. Catal.* **77,** 221 (1982); (b) Millman, W. S., Segawa, K., Smrz, D., and Hall, W. K., *Polyhedron* **5,** 169 (1986).
43. Segawa, K., Kim, D. S., Kurusu, Y., and Wachs, I. E., *in* "Proceedings, 9th International Congress on Catalysis, Calgary, 1988" (M. J. Phillips and M. Ternan, Eds.), p. 1960. Chem. Institute of Canada, Ottawa, 1988.
44. Aveston, J., and Anacker, E. W., and Johnson, J. S., *Inorg. Chem.* **3,** 735 (1964).
45. Honig, D. S., and Kustin, K., *Inorg. Chem.* **11,** 65 (1972).
46. Haihgt, G. P., and Boston, D. R., *in* "Proceedings, 1st International Climax Conference on the Chemistry and Uses of Molybdenum" (P. C. H. Mitchell, Ed), p. 48. London, 1973.
47. Ekerdt, J., Kohler, S. D., Kim, D. S., and Wachs, I. E., to be published.
48. Gil-Llambias, F. J., Escudey, A. M., Fierro, J. L. G., and Lopez Agudo, A., *J. Catal.* **95,** 520 (1985).

49. Vuurman, M. A., and Wachs, I. E., submitted for publication.
50. Brunelle, J. P., *Pure Appl. Chem.* **50,** 1211 (1978).
51. Leyrer, J., Vielhabor, B., Zaki, M. I., Zhuang, S., Weitkamp, J., Knozinger, H., *Mater. Chem. Phys.* **13,** 301 (1985).
52. Liu, T., Forissier, M., Coudurier, G., and Verdrine, J. C., *J. Chem. Soc., Faraday Trans. 1* **8,** 1607 (1989).
54. Tsigdinos, G. A., Chen, H. Y., and Streusand, B. J., *Ind. Eng. Chem. Prod. Res. Dev.* **20,** 619 (1981).
55. Caceres, C. V., Fierro, J. L. G., Lopez Agudo, A., Blanco, M. N., and Thomas, H. J., *J. Catal.* **95,** 501 (1985).